



Data Article

Dataset of geophysical electrical resistivity and subsurface profiling for natural resources exploration in a hard rock terrain of Tamil Nadu, India

Pradeep Kamaraj^{a,b,*}, Shankar Karuppanan^b^aDepartment of Biomaterials, Saveetha Dental College and Hospitals, SIMATS, Saveetha University, Chennai, 600077, India^bDepartment of Applied Geology, School of Applied Natural Sciences, Adama Science and Technology University (ASTU), Adama, 1888, Ethiopia

ARTICLE INFO

Article history:

Received 22 December 2023

Revised 2 March 2024

Accepted 5 March 2024

Available online 12 March 2024

Dataset link: [Geophysical resistivity data \(Original data\)](#)*Keywords:*

Geophysics

Vertical electrical sounding

CRM-500 Aquameter

IPI2WIN

Pseudo-section

ABSTRACT

Geophysical resistivity technique; vertical electrical sounding (VES)/earth resistivity test (ERT) was carefully done at 35 locations in a hard rock terrain of Tamil Nadu, India to evaluate natural resources such as groundwater, economic mineral deposits, etc., Data acquisition was done by CRM-500 Aquameter along with GPS, topographic map, Brunton compass, measuring tape, field notebook, hammer, iron rods (electrodes), and batteries. Furthermore, the major four subsurface layers' thickness, resistivity, and pseudo-section profiles were identified from the resistivity dataset using IPI2WIN. The resistivity curve type is also evaluated from the consecutive subsurface layers' resistivities. These can be helpful in groundwater potential zone identification studies. The entire dataset from this research can be useful in groundwater exploration, management, economic mineral exploration, waste disposal sites, reservoir, and dam site selections, and identifying the structural controls such as fractures, joints, buried anticlines, etc., The data also can be coupled with other regional geological and geophysical datasets for many natural resource exploration and exploitation studies.

* Corresponding author at: Department of Applied Geology, School of Applied Natural Sciences, Adama Science and Technology University (ASTU), Adama, 1888, Ethiopia.

E-mail addresses: pradeep.kamaraj@astu.edu.et, pradeep619rep@gmail.com (P. Kamaraj).

Specifications Table

| | |
|-----------------------|--|
| Subject | Geophysics. |
| Specific subject area | Electrical resistivity method |
| Data format | Raw data Processed data Images/Profiles |
| Type of data | Tables: subsurface layers thickness and resistivity data, resistivity curve types Figures: subsurface profiling |
| Data collection | The raw data was the electrical resistivities of subsurface layers. The resistivity values were measured by using CRM – 500 Aquameter, and Schlumberger's rods arrangement method. The resistivity is measured by the free flow of current to the subsurface and the potential difference from equipotential lines. The data can be used to evaluate the natural resources in the subsurface |
| Data source location | The dataset area is located between longitude 77°38'E and 78°3'E, latitude 11°37'N and 11°56'N and covered 686.11 km ² areal extent from Salem district, Tamil Nadu, India |
| Data accessibility | Repository name: Geophysical resistivity data Data identification number: https://data.mendeley.com/datasets/ccm76xs64y/2 Direct URL to data: Geophysical resistivity data - Mendeley Data |

1. Value of the Data

- The data are valuable for displaying the subsurface layers in geotechnical and engineering applications for the exploration and exploitation of natural resources such as groundwater, economic mineral deposits, and hydrocarbons [1].
- The dataset will be useful to assess the structural controls of underlying rock formations, such as cracks, joints, and unconformities, as well as to anticipate groundwater borehole depth for researchers and academics working in hydrogeology, mineral prospecting, geotechnical engineering, and other related subjects [2].
- The dataset can also be utilized for education, research, natural resource management activities, and policymakers in terms of identifying excessive groundwater withdrawals, which typically induce aquifer vulnerability [3–5].
- The data can be used for multipurpose applications in waste disposal sites, groundwater pollutions, recharge estimation, reservoirs as well as dam site selections by integrating with other geological and geophysical datasets [6,7]
- The data could populate a huge database or repository for regional geological, geophysical, and engineering investigations in the planned proposed area. Data scarcity has been cited as a barrier to conducting thorough regional natural resource exploration research in India.

2. Background

Stanley Reservoir and Mettur Dam have an impact on the intended region. As a result, more attention must be paid to engineering geological goals such as soil pipeline network identification. This data will be useful because it is non-destructive and is most effective at detecting soil pipeline networks to create tomography [8]. This information will also be utilized to assess the quality of subsoil and structural elements. Furthermore, the 1D photographs can aid in the creation of 2D and 3D subsurface models for acceptable drill location identification as well as groundwater prospecting views [9,10]. Also, the current dataset will be useful in identifying

the soil characteristics, fluid accumulation, and fluid quality in the subsurface. In addition, the data can be used to identify reliable inferences from historical maps especially in archaeological investigations [11,12]. The current work is designed to provide enormous chances to the audience, which includes researchers, academicians, and stockholders based on the benefits indicated above.

3. Data Description

The current work includes both raw data (electrical resistivities) and processed data such as thickness, subsurface layer resistivities, and pseudo-section profiles. The raw data includes GPS (Global Positioning System) information, as well as the thicknesses and resistivities of the four primary subsurface layers, including topsoil, weathered zone, first fracture zone, second fracture zone, and the curve type of each VES point. The pseudo-profiles show the vertical and lateral resistivity changes based on the places chosen.

4. Experimental Design, Materials and Methods

4.1. Research area

The present research area is an administrative boundary often called taluk (Mettur taluk) in Salem district, Tamil Nadu, India, located between longitude 77°38'E and 78°3'E, latitude 11°37'N and 11°56'N and covered 686.11 km² areal extent (Fig. 1). Fissile hornblende biotite gneiss (323.37 km²) and charnockite (307.6 km²) are the predominant rock types followed by

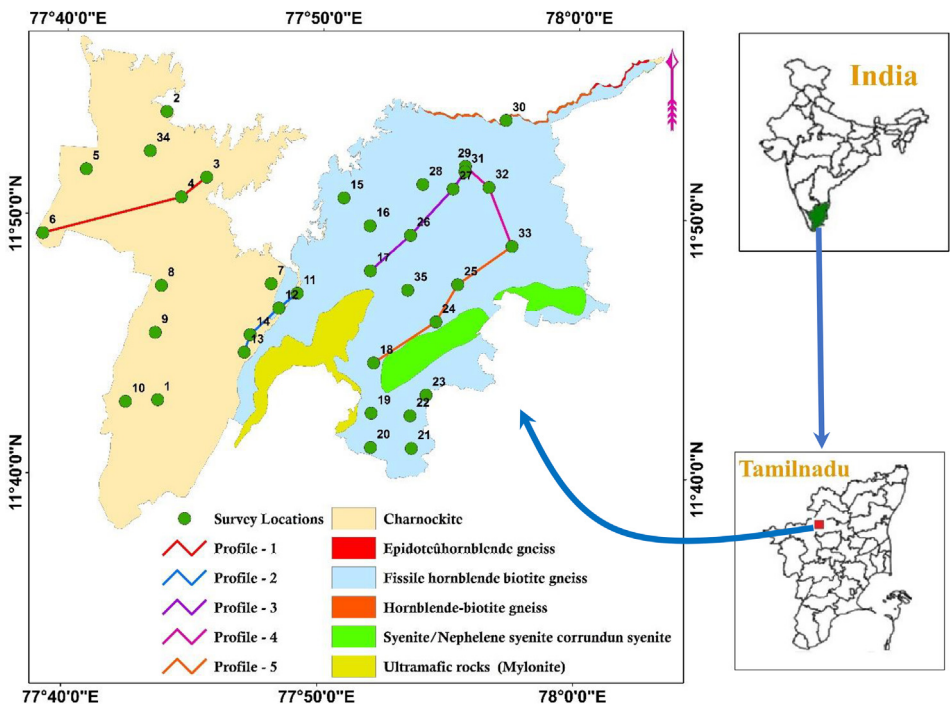


Fig. 1. Map showing the area of interest with lithological distribution, survey locations, and pseudo-profiles.

ultramafic mylonite (27.5 km²) and syenite rocks (25.14 km²). Generally, these rocks are mostly in weathered and/or fractured, and it is useful for groundwater recharge, and accumulation of natural resources within them. The temperature ranges from ~ 20 °C to 35 °C during winter and summer seasons with an average annual rainfall of 804 mm [13]. One of the major reservoirs in India namely, 'Stanley Reservoir' lies across the Cauvery River that flows from north to south, and this river is the primary water source for agricultural activities of Tamil Nadu's deltaic regions.

4.2. Data acquisition and processing

The resistivity data was acquired based on Schlumberger's electrode arrangements for 35 different locations selected from the topographic map by equal grid method. The location information (GPS) was noted for each VES before the instrumentation. Furthermore, the strike and dip directions were measured since the survey direction should be in the strike direction. Also, the survey locations were got rid of electrical, and underground pipelines to ensure that the received resistivity values were not affected by those hindrances. The CRM-500 Aquameter along with GPS, topographic map, Brunton compass, measuring tape, field notebook, hammer, iron rods (electrodes), and batteries were employed to do the entire geophysical survey. The survey was conducted with an extreme electrode distance of 150 m. A rope winch was fixed in the ground for 150 m before the survey to arrange all the electrodes in a straight line. There were five iron rods (electrodes), two current electrodes, two potential electrodes, and one central electrode used for the resistivity survey. There were two main components such as current electrode distance from the instrument ($AB/2$), and potential electrode distance from the instrument ($MN/2$) used to measure the resistivity. The resistivity meter was designed to measure the apparent resistivity of the subsurface layers by multiplying the geometric constant (K) and resistance of the earth material (R).

The resistivity dataset was then taken into the IPI2WIN platform to demarcate subsurface layer thickness, resistivity, and profiling. Three values $AB/2$, $MN/2$, and apparent resistivity (ρ) were used to evaluate the dataset. Furthermore, three potential keys such as split (to separate the layers), merge (to combine the layers), and inversion (to reduce the error percentage). The subsurface layers' thickness and resistivity were generated by fixing the movable red line with the stable black line. The error percentage was restricted to under 5% to ensure the quality of the dataset. Finally, the data table from IPI2WIN showed the subsurface layers' thickness as 'h' in 'm', and resistivities as ' ρ ' in ' $\Omega.m$ '. The curve type of resistivity sounding was identified by three consecutive layers resistivity values as: (Low-high-high = $\rho_1 < \rho_2 < \rho_3$ - 'A type', low-high-low = $\rho_1 < \rho_2 > \rho_3$ - 'K type', high-low-high = $\rho_1 > \rho_2 < \rho_3$ - 'H type', high-low-low = $\rho_1 > \rho_2 > \rho_3$ - 'Q type') [14,15]. All these subsurface layers' thickness, resistivity, and curve types are represented in Table 1. These curve-type data can be useful in the identification of groundwater potentiality.

There are five profiles presented in this research, and the locations for profiling were selected based on the groundwater flow direction. All the profiles are from northeast to southwest directions except profile 4. The figures (Figs. 2–6) represent the pseudo-section resistivity profiles of the proposed area. Because most of the region the groundwater flow was from north to south due to the presence of Stanley Reservoir in the central north portion [16]. So, the resistivity variation can be obtained from the colour ramp variation, the depth of the layer can be found from the y-axis values, and the distance of each location in the profile can be taken from the lateral x-axis values in the profiles. The lateral distances of each location in the profiles are represented in Table 2. These profile data can be utilized for three-dimensional (3-D) subsurface modelling.

These thickness, resistivity, and profile datasets will be used to evaluate the characteristics of horizontal or dipped rocks, economic mineral deposits such as placer/bedded deposits, recharge estimation, depth of the aquifer, structural controls such as buried anticlines, and various other engineering geological purposes.

Table 1

Detailed resistivity interpretation data of each VES point.

| VES No | Longitude | Latitude | Thickness in 'm', and Resistivity in 'Ω.m' | | | | | | | Curve type | |
|----------|-----------|----------|--|-------|-------|--------|-----------|---------|-----------|------------|------|
| | | | TT | WZT | FFZT | SFZT | TR | WZR | FFZR | | SFZR |
| VES - 1 | 77.73 | 11.71 | 0.66 | 0.13 | 1.84 | 97.40 | 22.90 | 991.00 | 50.10 | 1091.00 | KH |
| VES - 2 | 77.73 | 11.90 | 0.16 | 4.22 | 45.90 | 26.60 | 12.40 | 198.00 | 399.00 | 1941.00 | AA |
| VES - 3 | 77.76 | 11.86 | 0.44 | 0.52 | 1.65 | 76.10 | 27.00 | 797.00 | 38.30 | 468.00 | KH |
| VES - 4 | 77.74 | 11.84 | 2.00 | 13.00 | 45.00 | 40.00 | 7.69 | 33.76 | 136.36 | 175.43 | AA |
| VES - 5 | 77.68 | 11.86 | 1.55 | 14.70 | 8.98 | 122.00 | 58.40 | 58.70 | 16,355.00 | 303.00 | AK |
| VES - 6 | 77.65 | 11.82 | 2.00 | 1.03 | 9.94 | 86.90 | 43.00 | 22.50 | 57.70 | 1663.00 | HA |
| VES - 7 | 77.80 | 11.79 | 0.18 | 13.10 | 10.20 | 127.00 | 32.30 | 165.00 | 21,533.00 | 223.00 | AK |
| VES - 8 | 77.73 | 11.79 | 0.86 | 6.30 | 4.70 | 138.00 | 36.60 | 84.00 | 43,779.00 | 131.00 | AK |
| VES - 9 | 77.73 | 11.76 | 0.89 | 0.18 | 5.35 | 144.00 | 103.00 | 17.70 | 92.10 | 91,904.00 | HA |
| VES - 10 | 77.71 | 11.71 | 0.65 | 1.75 | 16.90 | 131.00 | 80.50 | 8.31 | 4756.00 | 1863.00 | HK |
| VES - 11 | 77.82 | 11.78 | 0.56 | 3.46 | 19.90 | 126.00 | 344.00 | 86.70 | 259.00 | 110.00 | HK |
| VES - 12 | 77.81 | 11.77 | 0.44 | 0.36 | 30.50 | 18.20 | 35.60 | 3366.00 | 141.00 | 3.14 | KQ |
| VES - 13 | 77.78 | 11.75 | 1.50 | 7.00 | 19.50 | 62.00 | 5.55 | 7.57 | 54.90 | 95.74 | AA |
| VES - 14 | 77.79 | 11.76 | 0.88 | 0.66 | 6.00 | 142.00 | 408.00 | 15.80 | 9853.00 | 23.20 | HK |
| VES - 15 | 77.85 | 11.85 | 3.22 | 0.97 | 2.49 | 143.00 | 61.80 | 202.00 | 21.20 | 55,767.00 | KH |
| VES - 16 | 77.86 | 11.83 | 2.50 | 10.00 | 45.00 | 45.50 | 6.94 | 26.32 | 132.18 | 239.53 | AA |
| VES - 17 | 77.87 | 11.80 | 3.00 | 19.50 | 25.00 | 23.50 | 14.28 | 39.82 | 131.94 | 179.75 | AA |
| VES - 18 | 77.87 | 11.74 | 1.50 | 13.50 | 14.00 | 11.00 | 16.67 | 26.84 | 60.00 | 71.30 | AA |
| VES - 19 | 77.87 | 11.71 | 0.57 | 3.54 | 96.50 | 48.90 | 248.00 | 23.90 | 11,794.00 | 142.00 | HK |
| VES - 20 | 77.87 | 11.69 | 0.89 | 8.15 | 42.50 | 95.40 | 70.70 | 335.00 | 831.00 | 48,014.00 | AA |
| VES - 21 | 77.89 | 11.68 | 0.84 | 1.30 | 2.56 | 66.70 | 310.00 | 3105.00 | 58.70 | 882.00 | KH |
| VES - 22 | 77.89 | 11.71 | 1.42 | 0.50 | 5.10 | 12.40 | 88.30 | 20.60 | 6984.00 | 183.00 | HK |
| VES - 23 | 77.90 | 11.72 | 2.00 | 10.50 | 26.50 | 11.00 | 25.00 | 80.65 | 185.71 | 217.39 | AA |
| VES - 24 | 77.91 | 11.77 | 0.67 | 5.48 | 7.49 | 75.00 | 367.00 | 144.00 | 3421.00 | 1221.00 | HK |
| VES - 25 | 77.92 | 11.79 | 3.00 | 7.25 | 5.75 | 34.00 | 6.73 | 16.13 | 25.81 | 80.65 | AA |
| VES - 26 | 77.89 | 11.82 | 2.50 | 17.50 | 10.00 | 20.00 | 2.76 | 20.97 | 51.72 | 79.36 | AA |
| VES - 27 | 77.92 | 11.85 | 0.56 | 0.37 | 18.10 | 108.00 | 147.00 | 6.78 | 130.00 | 33,601.00 | HA |
| VES - 28 | 77.90 | 11.85 | 0.22 | 3.86 | 61.10 | 85.20 | 42,035.00 | 109.00 | 4488.00 | 160,000.00 | HA |
| VES - 29 | 77.93 | 11.87 | 3.75 | 20.00 | 31.25 | 24.00 | 8.15 | 35.45 | 77.46 | 120.63 | AA |
| VES - 30 | 77.95 | 11.90 | 1.00 | 11.00 | 15.00 | 23.00 | 0.90 | 26.50 | 75.00 | 138.38 | AA |
| VES - 31 | 77.93 | 11.86 | 2.00 | 2.00 | 6.00 | 20.00 | 13.33 | 10.00 | 43.48 | 111.11 | HA |
| VES - 32 | 77.94 | 11.85 | 1.50 | 6.00 | 28.50 | 40.00 | 25.00 | 23.00 | 70.22 | 208.01 | HA |
| VES - 33 | 77.96 | 11.82 | 0.04 | 10.50 | 5.52 | 83.90 | 23.70 | 449.00 | 22,171.00 | 65.00 | AK |
| VES - 34 | 77.72 | 11.89 | 4.00 | 10.00 | 23.00 | 38.00 | 12.49 | 41.18 | 79.57 | 138.88 | AA |
| VES - 35 | 77.89 | 11.79 | 0.38 | 3.66 | 57.90 | 38.10 | 17.40 | 88.70 | 877.00 | 11,153.00 | AA |

(Note: TT – Topsoil thickness, WZT – Weathered zone thickness, FFZT – First fracture zone thickness, SFZT – Second fracture zone thickness, TR – Topsoil resistivity, WZR – Weathered zone resistivity, FFZR – First fracture zone resistivity, SFZR – Second fracture zone resistivity).

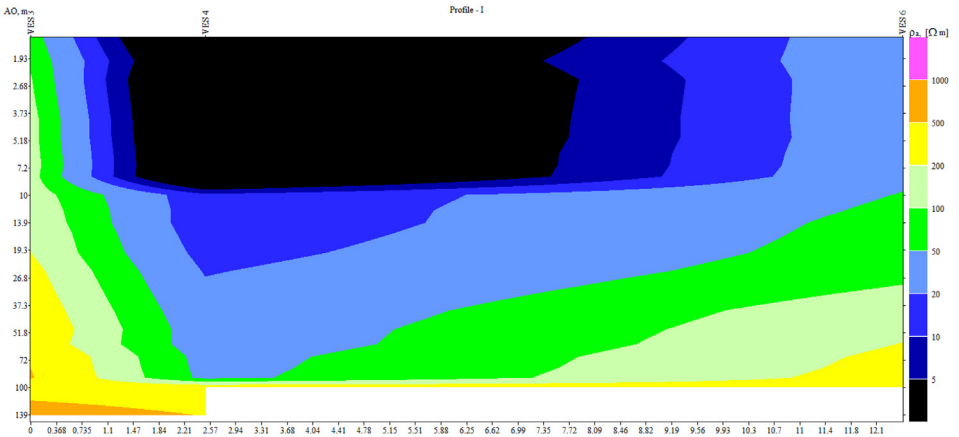


Fig. 2. 'Profile - 1' represents vertical depth variation, lateral distance, and resistivity variations.

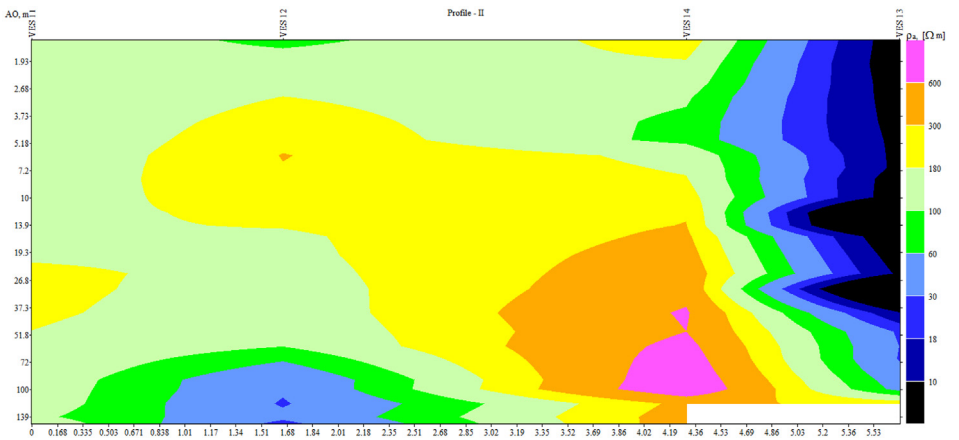


Fig. 3. 'Profile - 2' represents vertical depth variation, lateral distance, and resistivity variations.

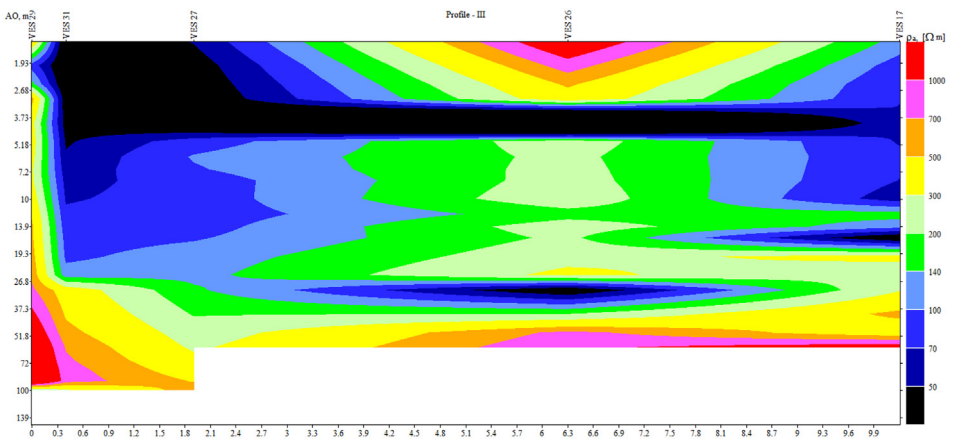


Fig. 4. 'Profile - 3' represents vertical depth variation, lateral distance, and resistivity variations.

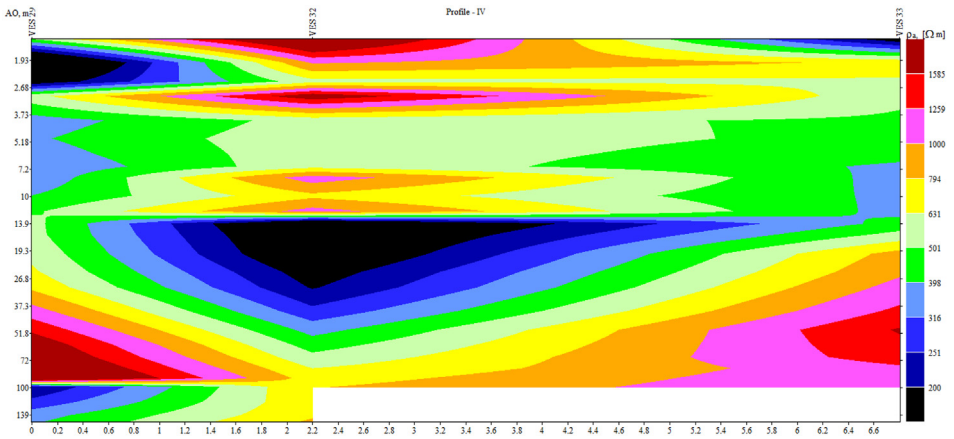


Fig. 5. 'Profile - 4' represents vertical depth variation, lateral distance, and resistivity variations.

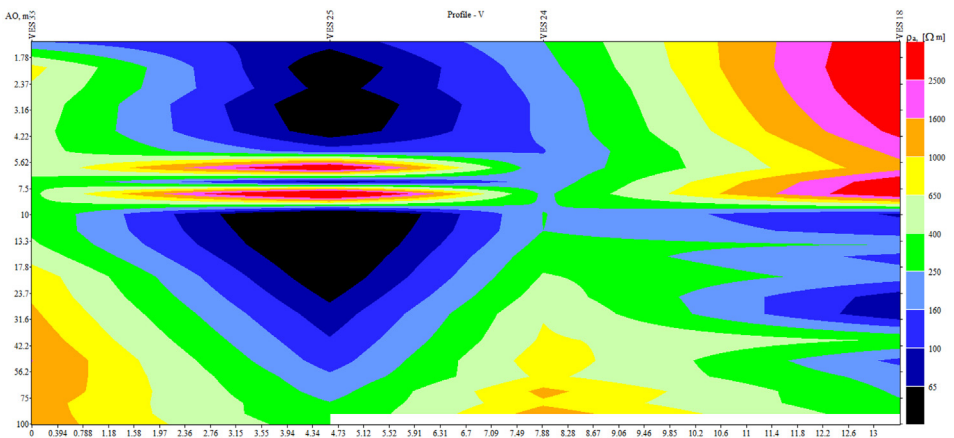


Fig. 6. 'Profile - 5' represents vertical depth variation, lateral distance, and resistivity variations.

Table 2
Pseudo-profile details.

| Profile | VES locations | Lateral distances in 'km' |
|-------------|--------------------|---------------------------|
| Profile - 1 | VES 3-4-6 | 0-2.5-12.5 |
| Profile - 2 | VES 11-12-14-13 | 0-1.65-4.3-5.7 |
| Profile - 3 | VES 29-31-27-26-17 | 0-0.4-1.9-6.3-10.2 |
| Profile - 4 | VES 29-32-33 | 0-2.2-6.8 |
| Profile - 5 | VES 33-25-24-18 | 0-4.6-7.9-13.4 |

Limitations

The maximum electrode distance of 150 m was adopted to acquire the dataset. But the distance was reduced in few locations due to the terrain conditions (undulations), vegetative cover, and urban infrastructure. These factors obstructed the actual plan of 40 locations by 15 km grid then reduced as 35 (as 20 km grid), and subsequently they influenced in the data interpretations. Also, there were five profiles have been made based on the groundwater flow direction. Furthermore, the dataset will be much beneficial especially in groundwater exploration, and engineer-

ing geological studies if the number of survey locations will be increased based on groundwater flow directions.

Ethics Statement

The authors have read and follow the [ethical requirements](#) for publication in Data in Brief and confirming that the current work does not involve human subjects, animal experiments, or any data collected from social media platforms.

Data Availability

[Geophysical resistivity data \(Original data\)](#) (Earth/Chem).

CRedit Author Statement

Pradeep Kamaraj: Conceptualization, Methodology, Investigation, Formal analysis, Software, Data curation, Validation, Visualization, Writing – review & editing; **Shankar Karuppannan:** Investigation, Formal analysis, Data curation, Validation, Visualization.

Acknowledgements

This research did not receive any specific grant from funding agencies in the public, commercial, or not-for-profit sectors.

Declaration of Competing Interest

The authors declare that they have no known competing financial interests or personal relationships that could have appeared to influence the work reported in this paper.

References

- [1] W.O. Raji, K.A. Abdulkadir, Geo-resistivity data set for groundwater aquifer exploration in the basement complex terrain of Nigeria, West Africa, *Data Br.* 31 (2020) 105975.
- [2] B. Panda, S. Chidambaram, N. Ganesh, An attempt to understand the subsurface variation along the mountain front and riparian region through geophysics technique in South India, *Model. Earth Syst. Environ.* 3 (2017) 783–797.
- [3] P. Kamaraj, C. Sabarathinam, M. Haji, P. Choudhury, A.I. Abdelpahman, M. Missionnaire, An integrated approach to evaluate the status of the coastal aquifer near the mouth of Coleroon River, Tamil Nadu, in: *Groundw. Contam. Coast. Aquifers*, Elsevier, 2022, pp. 105–118.
- [4] A.M. MacDonald, H.C. Bonsor, B.É.Ó. Dochartaigh, R.G. Taylor, Quantitative maps of groundwater resources in Africa, *Environ. Res. Lett.* 7 (2012) 24009.
- [5] A.P. Aizebeokhai, O. Ogungbade, K.D. Oyeyemi, Geoelectrical resistivity data set for characterising crystalline basement aquifers in Basiri, Ado-Ekiti, southwestern Nigeria, *Data Br.* 19 (2018) 810–816.
- [6] B. Panda, C. Sabarathinam, G. Nagappan, T. Rajendiran, P. Kamaraj, Multiple thematic spatial integration technique to identify the groundwater recharge potential zones—a case study along the Courtallam region, Tamil Nadu, India, *Arab. J. Geosci.* 13 (2020) 1–16.
- [7] B. Panda, S. Chidambaram, N. Ganesh, V.S. Adithya, K. Pradeep, U. Vasudevan, A.L. Ramanathan, S. Ranjan, M.V. Prasanna, K. Paramaguru, A study on mountain front recharge by using integrated techniques in the hard rock aquifers of southern India, *Environ. Dev. Sustain.* 20 (2018) 2243–2259.
- [8] M. Joshi, A. Gond, P.R. Prasobh, S. Rajappan, B.P. Rao, V. Nandakumar, Significance and limit of electrical resistivity survey for detection sub surface cavity: a case study from, Southern Western Ghats, India, in: *Basics Comput. Geophys.*, Elsevier, 2021, pp. 81–93.
- [9] M. Lech, Z. Skutnik, M. Bajda, K. Markowska-Lech, Applications of electrical resistivity surveys in solving selected geotechnical and environmental problems, *Appl. Sci.* 10 (2020) 2263.

- [10] I. Muchingami, D.J. Hlatywayo, J.M. Nel, C. Chuma, Electrical resistivity survey for groundwater investigations and shallow subsurface evaluation of the basaltic-greenstone formation of the urban Bulawayo aquifer, *Phys. Chem. Earth* 50 (2012) 44–51 Parts A/B/C.
- [11] A. Samouëlian, I. Cousin, A. Tabbagh, A. Bruand, G. Richard, Electrical resistivity survey in soil science: a review, *Soil Tillage Res.* 83 (2005) 173–193.
- [12] M.L. Hargrave, L.E. Somers, T.K. Larson, R. Shields, J. Dendy, The role of resistivity survey in historic site assessment and management: an example from Fort Riley, Kansas, *Hist. Archaeol.* 36 (2002) 89–110.
- [13] P. Kamaraj, M. Jothimani, B. Panda, C. Sabarathinam, Mapping of groundwater potential zones by integrating remote sensing, geophysics, GIS, and AHP in a hard rock terrain, *Urban Clim.* 51 (2023) 101610.
- [14] A.O. Fajana, Groundwater aquifer potential using electrical resistivity method and porosity calculation: a case study, *NRIAG J. Astron. Geophys.* 9 (2020) 168–175.
- [15] S. Selvam, 1D Geoelectrical resistivity survey for groundwater studies in coastal area: a case study from Pearl City, Tamil Nadu, *J. Geol. Soc. India.* 87 (2016) 169–178.
- [16] K. Srinivasamoorthy, S. Chidambaram, M.V. Prasanna, M. Vasanthavihar, J. Peter, P. Anandhan, Identification of major sources controlling groundwater chemistry from a hard rock terrain—a case study from Mettur taluk, Salem district, Tamil Nadu, India, *J. Earth Syst. Sci.* 117 (2008) 49–58.